Published by Avanti Publishers

International Journal of Petroleum Technology

ISSN (online): 2409-787X

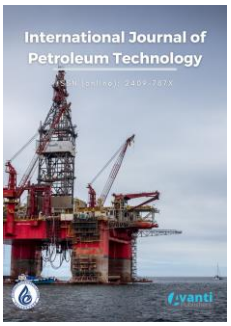

Prediction of the Dynamic Viscosity of N-Alcohol by Three Intelligent Models (ANN, LSSVM, and ANFIS) in Operation Conditions

Hossein Rajabi Kuyakhi[1] and Ramin Tahmasebi Boldaji[2,*]

[1]*Department of Chemical Engineering, University of Guilan, Rasht 41996-13769, Iran*

[2]*Department of Chemical Engineering, College of Engineering, University of Isfahan, Isfahan 81746-73441, Iran*

ARTICLE INFO

Article Type: Research Article

Keywords:
N-Alcohol
Taylor diagram
Dynamic viscosity
Artificial neural network (ANN)
Adaptive neuro-fuzzy inference system (ANFIS)
Least squares support vector machine (LSSVM)

Timeline:
Received: November 10, 2022
Accepted: December 14, 2022
Published: December 19, 2022

Citation: Kuyakhi HR, Boldaji RT. Prediction of the dynamic viscosity of n-alcohol by three intelligent models (ANN, LSSVM, and ANFIS) in operation conditions. Int J Petrol Technol. 2022; 9: 80-90.

DOI: https://doi.org/10.15377/2409-787X.2022.09.9

ABSTRACT

Viscosity is an essential property in chemical engineering for different applications. If predicted accurately, the viscosity has a significant effect on chemical applications. In this paper, the capability of the three intelligence models, artificial neural network (ANN), least squares support vector machine (LSSVM), and adaptive neuro-fuzzy inference system (ANFIS), were evaluated to model the dynamic viscosity of n-alcohol at the different operational conditions. The models were improved based on a 237 data set collected from reliable articles. The used databank contains temperature (T), pressure (P), and carbon number of n-alcohols (n-C) were chosen as the input of models. The result of these models was studied by Statistical parameters such as Mean of the squares errors (MSE), Root mean of the squares errors (RMSE), Maximum absolute error (MAAE %), Mean absolute error (MEAE %), correlation coefficient and graphical technique like Taylor diagram and William plot. The proposed models are known to appropriately estimate the viscosity of n-alcohol at the different operational conditions. It was found that the ANN with R2= 0.999, MSE=0.000017, MAAE %= 1.6, MEAE %=0.32 for Test, and R2= 0.999, MSE=0.0000094, MAAE %= 0.83, MEAE %=0.23 for Train exhibited a high performance than LSSVM and ANFIS for predicting dynamic viscosity of n-alcohol at the operational conditions.

*Corresponding Author
Email: Ramintahmasbi68@gmail.com
Tel: +(98) 9130844478

1. Introduction

Thermodynamic properties are important parameters in various areas of industry and science for pure materials and mixtures. Determination of viscosity and density are essential for usages such as heat and mass transfer and specification of flow in pipes. Alcohols have a key role in industrial applications; some were used as a solvent for fats, oils, resins, paints, and nitrocellulose applications [1]. The thermophysical alcohol mixture properties at different temperatures are essential in the cryogenics design power generation technique [2].

The study of viscosity determination of n-alcohols has been less commonly performed. Cano-Gómez *et al*. studied a correlation method to determine the viscosity of n-alcohols by The Tait equation [3]. Sülzner *et al*. measured the viscosities at different conditions, temperature (298-413k), and pressure (>195 mpa) [4]. Guzmán-López *et al*. presented the densities and viscosities of binary mixtures with carbon atoms from C7 toc10 [4]. Due to the difficulty in measuring liquid viscosities under high operational conditions (temperature and pressure), the experimental data are limited [5]. There are commonly two approaches to estimating such parameters, i.e., The thermodynamic approaches and intelligence models. Machin learning approaches make relations between inputs and outputs without considering difficult thermodynamic concepts [6]. The intelligence method is usually divided into four parts: the Fuzzy Logic System, artificial neural network, support vector Machine, and adaptive neuro-fuzzy [7-10].

Learning approaches have been investigated for forecasting the viscosity of the fluid. Elham Heidari *et al*. studied nanofluid viscosity by a multilayer perceptron artificial neural network. [11] Eghtedaee *et al*. investigated the radial basis function artificial network to predict the viscosity of mixed oil [7]. Davood Toghraie *et al*. designed an ANN to estimate the viscosity of Silver/Ethylene glycol nanofluid at various temperatures [12]. Hao Chen *et al*. studied an ANN to estimate the viscosity of microalgae slurry in a hydrothermal hydrolysis process [13]. Based on our knowledge, there is no study on n-alcohol solvent viscosity modeling in operation conditions. Thus, in this article, the artificial intelligence approaches, namely ANN, LSSVM, and ANFIS, are proposed to estimate the viscosity of n-alcohol at different operation conditions. The models were developed based on temperature, pressure, and carbon number of n-alcohol [14].

2. Methodology

2.1. Data Processing

It is considered that the dynamic viscosity of n-alcohol in operation conditions (Vs., μpa.s) is a function of the type of alcohol in the aqueous media (Cn, n), pressure of the system (P, Mpa), and the temperature (Tc, °C). As mentioned, the models were developed through 237 sample points of dynamic viscosities gathered from reliable papers [14]. The range of the data set is represented in Table **1**. In computational analysis, data normalization is a

crucial stage. Data normalization must be performed to neutralize the dimensional impacts of the parameters. The dataset was normalized between 0,1. The normalization data are obtained as follows:

$$a_i = \frac{a - a_{\min}}{a_{\max} - a_{\min}} \tag{1}$$

Table 1: The dilates of collected dataset.

N-Alcohols	Temperature (K)	Pressure (mpa)	Dynamic Viscosity (μpa.s)
1-Butanol	298-323-14	1.99-30.01	3287.1-1420.5
1-pentanol	298-323-14	1.98-30.2	4576.6-1832.9
1-Heptanol	298-323-14	1.99-30.1	56509-2748.5
1-Octanol	298-323-14	1.97-30.02	9865.9-3427.2
1-Nonanol	298-323-14	1.99-30.02	12513-4343.4

Where a_i is a set of normalized samples, a is actual data, a_{min} and a_{max} are lower and upper bond of set point. To develop the model processing, 70% of the data set was taken for training and 30% for the Test of performance models.

2.2. Adaptive Neuro-Fuzzy Inference System (ANFIS)

ANFIS was introduced as a smart hybrid technique by Jang [13]. Incorporating the fuzzy rules and the training laws makes more attention to this method [10]. The ANFIS structure has five layers shown with their equations in Fig (**1**). The Sugeno type of ANFIS can be described below:

$$\text{First rule: if } Y_1 \text{ is } z_1 \text{ and } Y_2 \text{ is } t_1, \text{ Then } f_1=P_1Y_1+q_1y_2+R_1$$
$$\text{Second rule: if } Y_1 \text{ is } z_1 \text{ and } Y_2 \text{ is } t_2, \text{ Then } f_2=P_2Y_1+q_2y_2+R_2 \quad (2)$$

As seen in Fig. (**1**), a fuzzy set of input data are obtained in the first layer, called the fuzzification layer. In the next step (rule layer), the model's output is obtained by considering the membership function. The firing strength ratio of the ith rule achieves in the normalization layer. Then, after defuzzification, the output obtains [15].

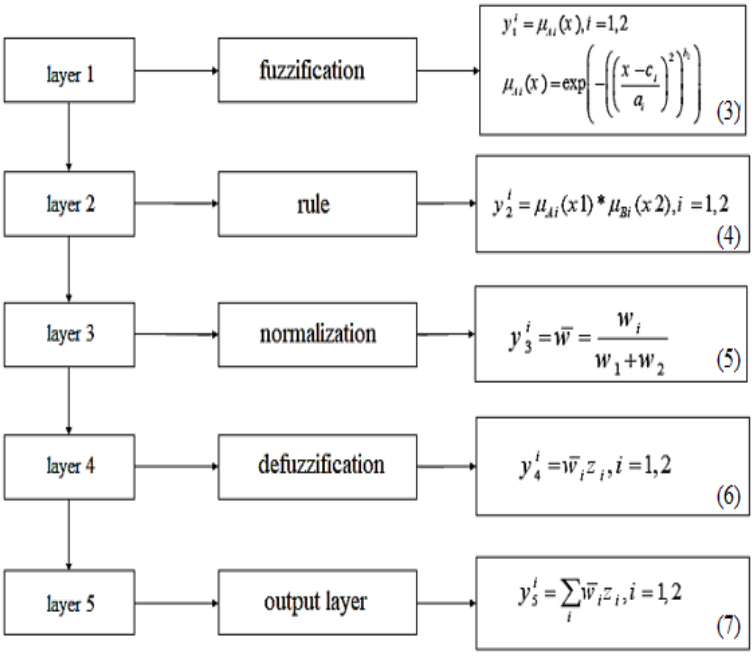

Figure 1: The *ANFIS* layers structure.

2.3. Artificial Neural Network (ANN)

ANN structure comprises three main layers: input, hidden, and output [16]. The layers are connected predicated on the computing unit called neurons [17, 18]. The transfer function (TF) is the main part of this model. There are various types of TF, such as Hyperbolic Tangent Sigmoid function (Tansig), and linear transfer function (Purelin), Log Sigmoid transfer function (Logsig) [19-21]. The backpropagation algorithm was commonly used to learn the network. The best result was defined by considering the correct number of neurons, the suitable number of hidden layers, the best training procedure, and transfer functions [22, 23].

2.4. LSSVM

The SVM is a learning model presented in the nineties, and it is used for classification and regression analysis. Simplicity and process speed are particular benefits of it. Solving a complex quadratic programming problem is required for the execution of the SVM technique, which makes a significant disadvantage of this technique [24].

LSSVM, an improved version of the SVM, is used to resolve this problem. More information about LSSVN is founded in [25, 26].

2.5. Statistical Analysis and Visualization

Based on Fig. (**2**), the dynamic viscosity is correlated with operation conditions, including pressure, temperature, and n-alcohol type. Fig. (**2**) represents the weight correlation of the Vs. with the input variables. It is observed that type of n-alcohol has the highest correlation value (0.60) with dynamic viscosity.

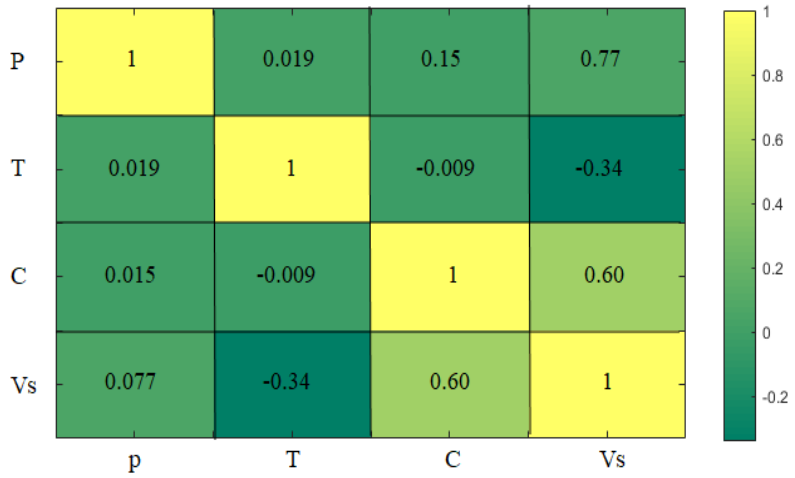

Figure 2: Correlation matrix of the input and output variables.

The scatter plot indicates linear behavior between Vs. and the input variable, shown in Fig. (**3**). From Fig. (**3**), alcohol type shows a low positive correlation, the temperature has a low negative correlation, and pressure has no significant correlation on dynamic viscosity.

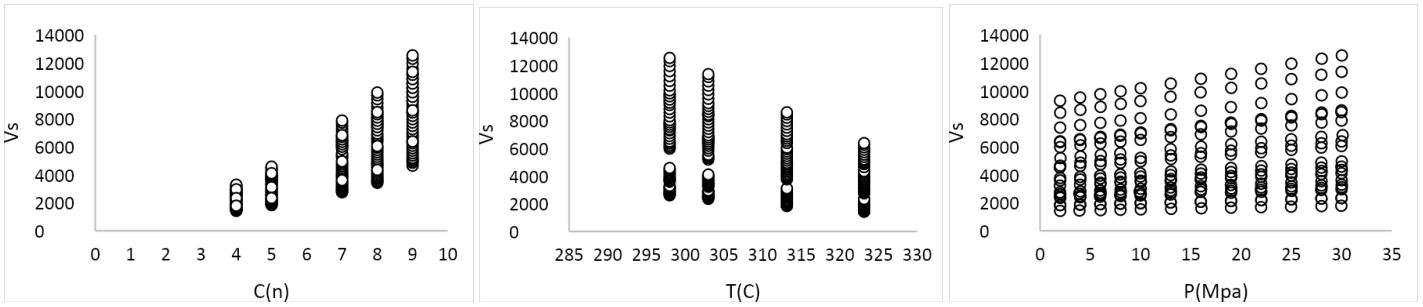

Figure 3: Illustration of scatter plots.

3. Result and Discussion

Learning models ANN, ANFIS, and LSSVM are developed for predicting the dynamic viscosity of n-alcohol at operation conditions. After data processing, the training dataset is used to train the LSSVM, ANFIS, and ANN. For ANN, the optimum weight and bias are obtained by one hidden neuron layer. The trial-and-error method was applied to reach the best structure of the models. Table **2** represents the optimum parameters of developed models.

To evaluate the accuracy of the established models for forecasting the dynamic viscosity of n-alcohol in operation conditions, performance parameters consist of Mean of the squares errors (MSE)**,** Root mean of the squares errors (RMSE)**,** Maximum absolute error (MAAE %)**,** Mean absolute error (MEAE %)**,** correlation coefficient are used. The expression of the performance parameters are given in Eq. 8 through Eq. 12.

Table 2: Specification of the ANN, ANFIS, and LSSVM.

	ANN	ANFISA	LSSVM
Number of inputs	3	3	3
Number of outputs	1	1	1
Fuzzy structure	-	Sugeno-type	-
Membership function type	-	Gaussian	-
Output membership function	-	Linear	-
Step size decrease rate	-	0.5	-
Step size increase rate	--	0.95	-
Number of output MF		6	-
Optimization method	trainlm	Hybrid	CSA
Neuron of hidden layer	4	-	-
Transfer function	tansig	-	-
Kernel function	-	-	RBF
σ^2	-	-	0.1

$$MSE = \frac{\sum_{i=1}^{k}(a-p)^2}{k} \tag{8}$$

$$RMSE = \sqrt{\frac{1}{k}\sum_{i=1}^{k}(a-p)^2} \tag{9}$$

$$MEAEP\% = \frac{1}{k}\sum_{i=1}^{k}\frac{|p-a|}{a} * 100 \tag{10}$$

$$MAAEP\% = \frac{\max|P-a|}{a} * 100 \tag{11}$$

$$R^2 = \frac{\sum_{i=1}^{n}(P_P - \bar{P})^2}{\sum_{i=1}^{n}(P_M - \bar{P}_M)^2} \tag{12}$$

Table **3** summarizes the performance parameters (i,e. *MSE, RMSE, MAAE%*, and *MEAE*) for the developed LSSVM, ANN, and ANFIS models. Typically, the correlation coefficient ranges between 0-1. This parameter shows that dataset on the regression. R^2 indicates that the model's dynamic viscosity can be estimated from the independent variables for all presented models. Fig. (**4f**) shows the output of the proposed models against experimental quantities of dynamic viscosities for the test and train stage. As shown, ANN has the best performance to fit the predicted values with measured data for test and train values.

From Table **3**, the calculated values of error parameters show that all the trained models for this aim can regenerate the goals with acceptable accuracy. However, the ANN model with MSE= 0.000017, MEAE= 0.32and MAAE=1.66 for test values provides better estimations.

Table 3: Performance of the ANN, ANFIS, and LSSVM based on statistical values.

Models	Test				
	MSE	**MEAE%**	**MAAE%**	R^2	**RMSE**
LSSVM	0.0018	3.28	14.7	0.990	0.042
ANFIS	0.00048	1.62	6.05	0.995	0.0221
ANN	0.000017	0.32	1.66	0.999	0.0042
	Train				
Models	MSE	MEAE%	MAAE%	R^2	RMSE
LSSVM	0.0021	3.37	19.82	0.988	0.045
ANFIS	0.00053	1.76	8.02	0.995	0.0232
ANN	0.0000094	0.23	0.83	0.999	0.0031

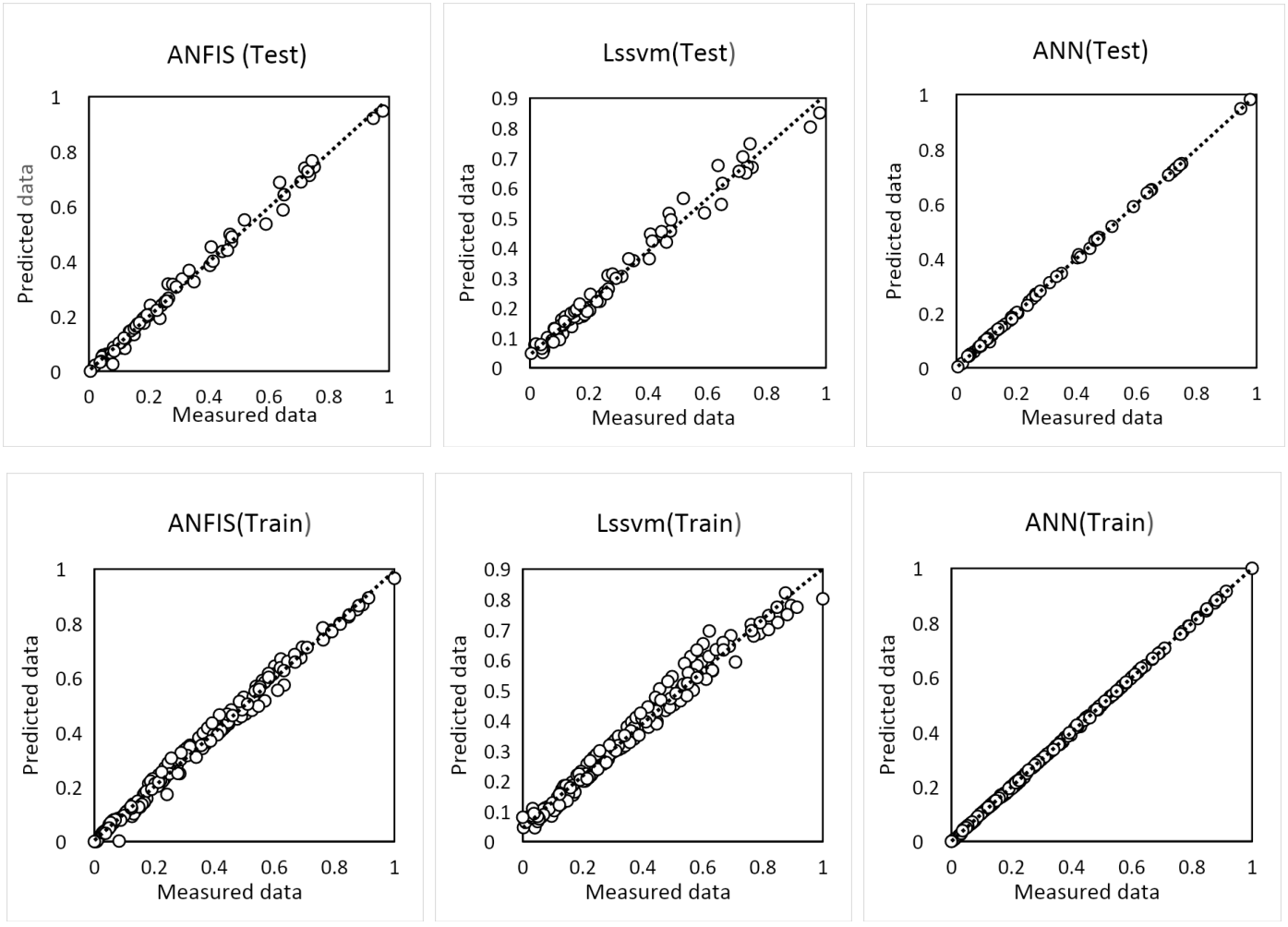

Figure 4: Regression plots for the train and test quantities.

Taylor diagram uses as a technique for indicating the validity of different models. In this plot, a target point shows the coefficient of correlation, the root-mean-square difference, and the ratio of the standard deviations. The point near the 'reference point' refers to the suitable learning model [27]. The Taylor diagram of the three developed models are shown in Fig. (**5**). The ANN model position point represented the best capability of this model.

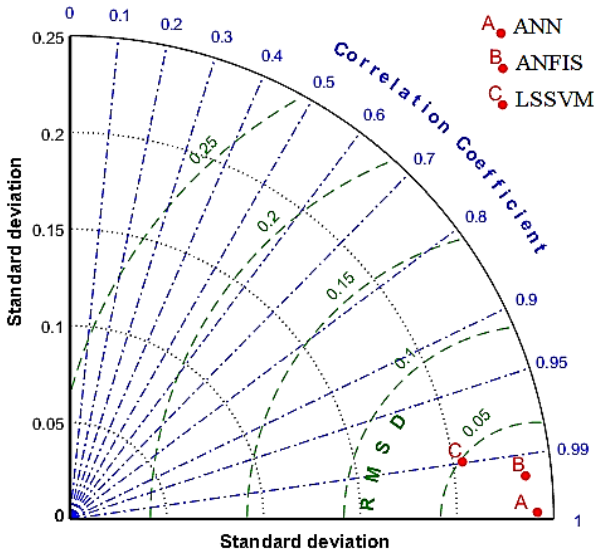

Figure 5: Taylor diagram of different models.

Regression error characteristic (REC) curve was used to evaluate the model performance. When the situation of the corresponding plot is near the left corner from the top, it represents the high reliability of the model [28]. The quantities of the area under the curve (AUC) are defined to measure the model's overall validity. Fig. (**6**) illustrates the REC curve for train and test data. As can be seen, the ANN model with AUC 0.9838 and 0.9939 for Test and training, respectively, is the best.

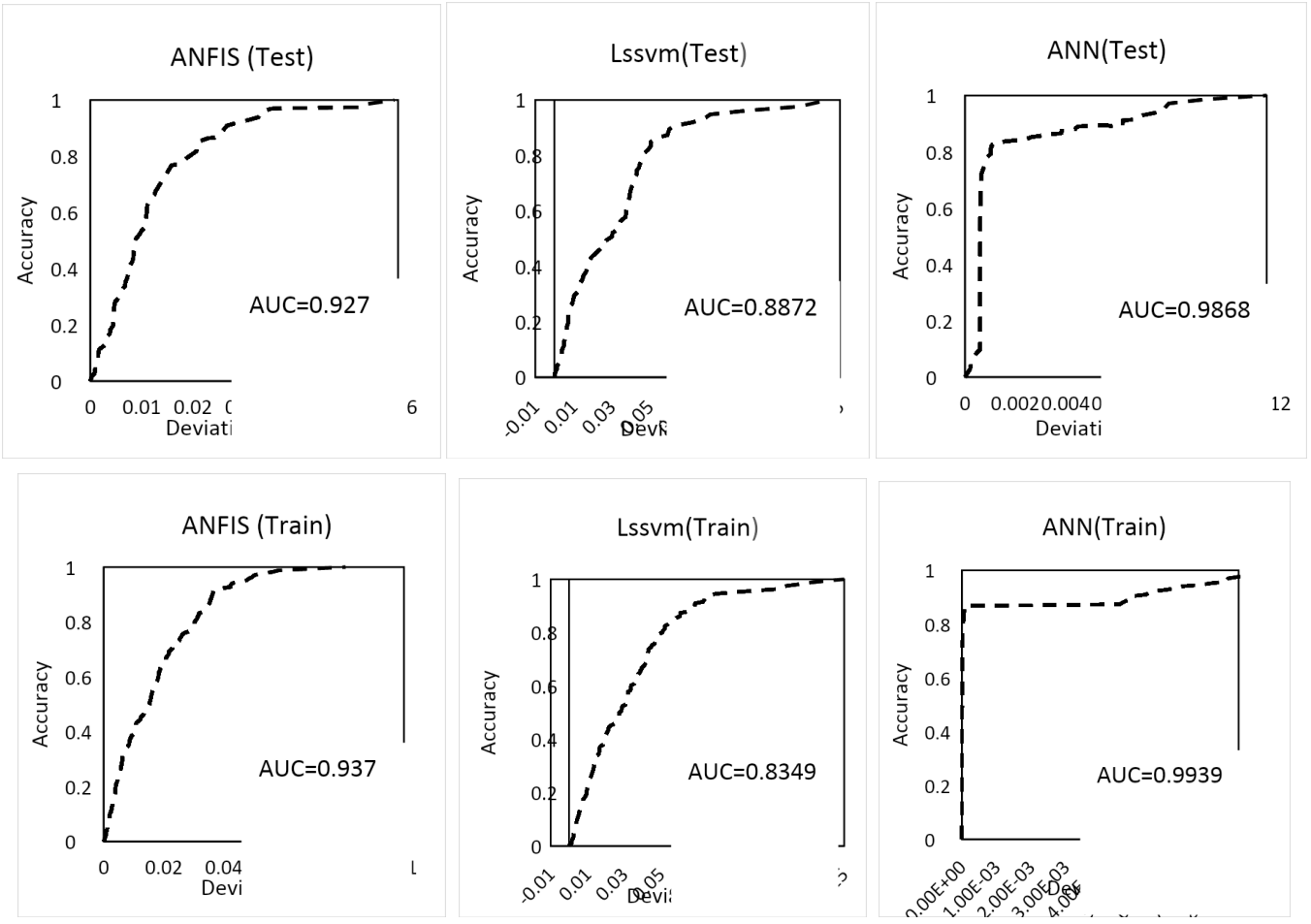

Figure 6: REC plot for Test and train.

An accuracy matrix was employed to assess the performance of the models Fig. (**7**). The matrix was formed of various performance parameters based on test and train data for evaluating the model's ability. In this technique, the reliability of the models is shown by comparing the performance variables to their ideal quantities, which are given by

$$u_e = \left|(1-\left|o_e\right|)\right| \times 100 \tag{13}$$

$$u_t = \frac{\left|o_a\right|}{l_a} \times 100 \tag{14}$$

Where u_e is accuracy for the error and u_t is the trend measuring parameters, and l_a la is the ideal value of parameters, O_e is an error (i,e. *MSE, RMSE, MAAE%*, and *MEAE*) and O_e trend (R^2) measuring parameters.

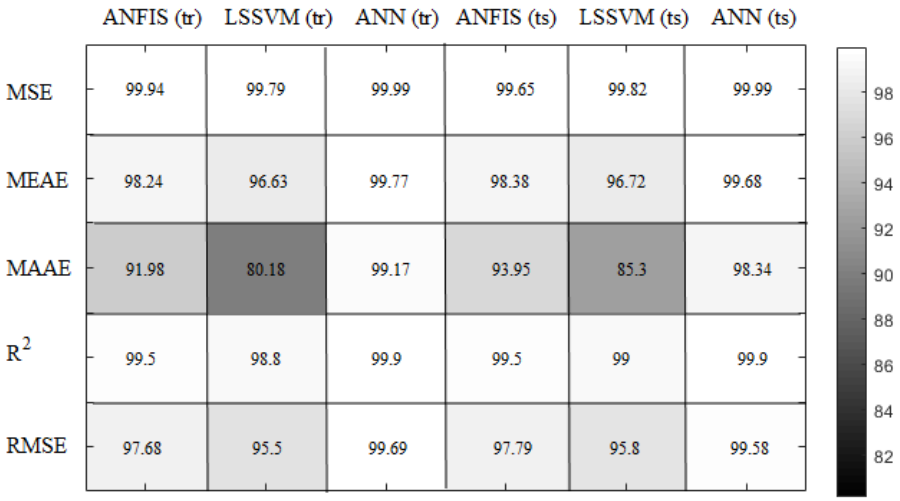

Figure 7: Accuracy Matrix of the models for training and testing stages.

Also, the reliability of the proposed models was investigated by the applicability domain (AD) approach [29]. There is a high possibility of existing outlier data in the measurement of the experimental process in mathematical models that include data collection, which may damage the accuracy of models [30]. A William diagram was taken for the illustration of an outlier. In this case, standard residual values were used in horizontal axes and leverage amounts in vertical axes. The Hat matrix is a symmetric matrix that makes a connection between predicted and real data shown as follows [29].

$$\hat{y}_i = Hy_i \tag{15}$$

Where y^i is estimated value, H is Hat matrix, yi is the actual value, and the Hat matrix is obtained by:

$$H = X\,(X^T X)^{-1} X^T \tag{16}$$

X is an (n*m) matrix, and H is a symmetric matrix (m*m), in which n and m are the data count and parameter, respectively. H* afford from 3*(k+1)/l, where k is the parameters count, and l refers to the count of data points [31, 32]. The applicability domain is n 0≤H≤H* and between the standardized residual ±3 [32].

In Fig. (**8**), the leverage approach was employed to detect outliers of the ANFIS model. The authoritative data points are set in the area within the range 0-H*. As can be seen, two outliers were found for ANFIS and LSSVM. ANN shows a high ability to configure between output data and input parameters with high accuracy with any outlier.

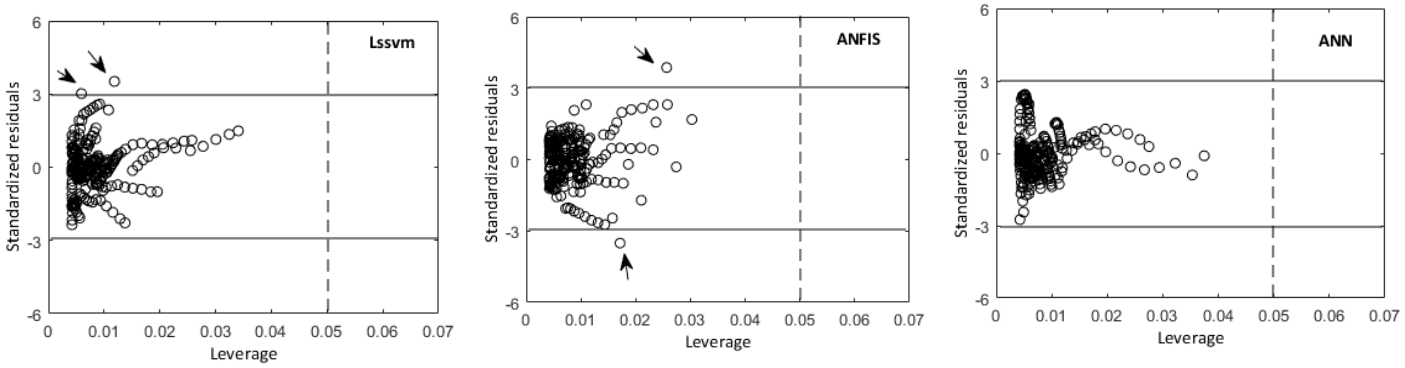

Figure 8: William plot.

3.1. Sensitivity Analysis (SA) and AIC

SA was used to determine the impact of independent parameters on the proposed model. The relevancy index of each independent variable was gathered from Eq 15. Where x_{il} denotes *lth* input, x_i is the Mean of the input, t_l related to *lth* output, and t is the Mean of output [33]. From Fig. (**9**), the n-alcohol type and temperature influence the model performance with 57 and 32 percent, respectively.

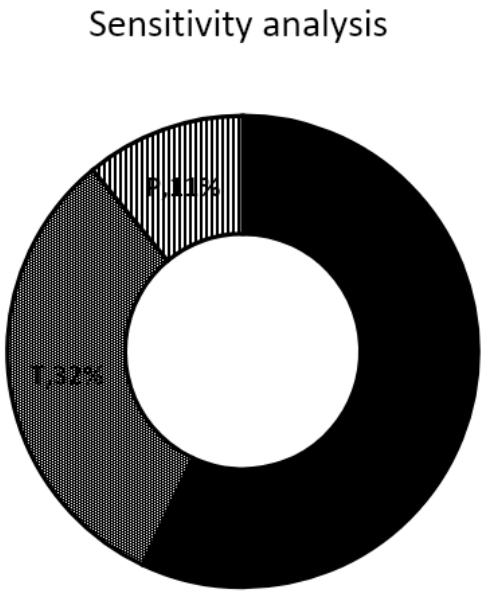

Figure 9: Sensitivity analysis.

$$R = \frac{\sum_{l=1}^{m}(x_{i,l} - \overline{x_i})(t_l - \bar{t})}{\sqrt{\sum_{l=1}^{m}(x_{i,l} - \overline{x_i})^2 \sum_{l=1}^{m}(t_l - \bar{t})^2}} \quad (17)$$

Also, an Akaike information criterion (AIC) was applied to compare the efficiency of the established models. The AIC result is represented in Table **4**. The smallest value of this index represents the best model [34, 35]. As can be seen, the ANN has the lowest value of this index. The AIC is defined by:

$$AIC = 2m - 2\ln\left(\sqrt{\frac{1}{k}\sum_{i=1}^{k}(a-p)^2}\right) \quad (18)$$

Table 4: Details of AIC value.

Models	AIC
LSSVM	17.21
ANFISA	13.55
ANN	12.36

4. Conclusion

In this study, the adequacy of the proposed models (i.e., ANN, ANFIS, and LSSVM) was appraised to forecasting the dynamic viscosity of n-alcohol. The actuarial parameters like MSE, R^2, RMSE, MAAEP%, and MEAEP% and graphical procedure (i.e., Taylor diagram, REC curve, and William plot) are utilized to investigate the behavior of the models. The outcome showed an acceptable capability of three models to anticipate the dynamic viscosity of n-alcohol, although the ANN model has the best performance in comparison to other suggested models. According to the results (i.e., R^2= 0.999, *MSE*=0.0000094, *MAAE* %= 0.83, *MEAE* %=0.23 for train data, and R^2= 0.999, *MSE*=0.000017, *MAAE* %= 1.6, *MEAE* %=0.32 for test data), the ANN can be considered as an appropriate technique for modeling the dynamic viscosity of n-alcohol.

References

[1] Cano-Gómez JJ, Iglesias-Silva GA, Ramos-Estrada M, Hall KR. Densities and viscosities for binary liquid mixtures of Ethanol + 1-Propanol, 1-Butanol, and 1-Pentanol from (293.15 to 328.15) K at 0.1 MPa. J Chem Eng Data. 2012; 57: 2560-7. https://doi.org/10.1021/je300632p

[2] Kumagai A, Yokoyama C. Liquid viscosity of binary mixtures of methanol with Ethanol and 1-Propanol from 273.15 to 333.15 K. Int J Thermophys. 1998; 19: 3-13. https://doi.org/10.1023/A:1021438800094

[3] Cano-Gómez JJ, Iglesias-Silva GA, Ramos-Estrada M. Correlations for the prediction of the density and viscosity of 1-alcohols at high pressures. Fluid Phase Equilib. 2015; 404:109-17. https://doi.org/10.1016/j.fluid.2015.06.042

[4] Guzmán-López A, Iglesias-Silva GA, Reyes-García F, Estrada-Baltazar A, Ramos-Estrada M. Densities and viscosities for binary liquid mixtures of n-undecane + 1-Heptanol, 1-Octanol, 1-Nonanol, and 1-Decanol from 283.15 to 363.15 K at 0.1 MPa. J Chem Eng Data. 2017; 62: 780-95. https://doi.org/10.1021/acs.jced.6b00834

[5] Matsuo S, Makita T. Viscosities of six 1-Alkanols at temperatures in the range 298? 348 K and pressures up to 200 MPa. Int J Thermophys. 1989; 10: 833-43. https://doi.org/10.1007/BF00514479

[6] Abdi-Khanghah M, Bemani A, Naserzadeh Z, Zhang Z. Prediction of solubility of N-alkanes in supercritical CO_2 using RBF-ANN and MLP-ANN. J CO_2 Util. 2018; 25: 108-19. https://doi.org/10.1016/j.jcou.2018.03.008

[7] Eghtedaei R, Abdi-khanghah M, Najar BSA, Baghban A. Viscosity estimation of mixed oil using RBF-ANN approach. Pet Sci Technol. 2017; 35: 1731-6. https://doi.org/10.1080/10916466.2017.1365084

[8] Baghban A, Namvarrechi S, Phung LTK, Lee M, Bahadori A, Kashiwao T. Phase equilibrium modelling of natural gas hydrate formation conditions using LSSVM approach. Pet Sci Technol. 2016; 34: 1431-8. https://doi.org/10.1080/10916466.2016.1202966

[9] Baghban A, Ahmadi MA, Hashemi Shahraki B. Prediction carbon dioxide solubility in presence of various ionic liquids using computational intelligence approaches. J Supercrit Fluids. 2015; 98: 50-64. https://doi.org/10.1016/j.supflu.2015.01.002

[10] Amin JS, Kuyakhi HR, Kashiwao T, Bahadori A. Development of ANFIS models for polycyclic aromatic hydrocarbons (PAHs) formation in sea sediment. Pet Sci Technol. 2019; 37: 679–86. https://doi.org/10.1080/10916466.2018.1563613

[11] Heidari E, Sobati MA, Movahedirad S. Accurate prediction of nanofluid viscosity using a multilayer perceptron artificial neural network (MLP-ANN). Chemom Intell Lab Sys. 2016; 155: 73-85. https://doi.org/10.1016/j.chemolab.2016.03.031

[12] Toghraie D, Sina N, Jolfaei NA, Hajian M, Afrand M. Designing an Artificial Neural Network (ANN) to predict the viscosity of Silver/Ethylene glycol nanofluid at different temperatures and volume fraction of nanoparticles. Phys A: Stat Mech Appl. 2019; 534(15): 122142. https://doi.org/10.1016/j.physa.2019.122142

[13] Chen H, Fu Q, Liao Q, Zhu X, Shah A. Applying artificial neural network to predict the viscosity of microalgae slurry in hydrothermal hydrolysis process. Energy AI. 2021; 4: 100053. https://doi.org/10.1016/j.egyai.2021.100053.

[14] Pimentel-Rodas A, Galicia-Luna LA, Castro-Arellano JJ. Viscosity and density of n-Alcohols at Temperatures between (298.15 and 323.15) K and Pressures up to 30 MPa. J Chem Eng Data. 2018; 64: 324-36. https://doi.org/10.1021/acs.jced.8b00812

[15] Kuyakhi HR, Boldaji RT. Developing an adaptive neuro-fuzzy inference system based on particle swarm optimization model for forecasting Cr (VI) removal by NiO nanoparticles. Environ Prog Sustain Energy. 2021; 40(4): e13597. https://doi.org/10.1002/ep.13597

[16] Taghavi H, Taghavi H. Proposing a novel and accurate model for forecasting dynamic viscosity of *n* -alkane in operational conditions. Pet Sci Technol. 2018; 36: 1531-6. https://doi.org/10.1080/10916466.2018.1476537

[17] Kuyakhi HR, Boldaji RT. A novel ANFIS model to prediction of the density of n-alkane in different operational condition. Pet Sci Technol. 2019; 37: 2429-34. https://doi.org/10.1080/10916466.2019.1616756

[18] Soroush E, Shahsavari S, Mesbah M, Rezakazemi M. A robust predictive tool for estimating CO_2 solubility in potassium based amino acid salt solutions. Chin J Chem Eng. 2018; 26 (4): 740-6. https://doi.org/10.1016/j.cjche.2017.10.002

[19] Baghban A, Ahmadi MA, Shahraki BH. Prediction carbon dioxide solubility in the presence of various ionic liquids using computational intelligence approaches. J Supercrit Fluids. 2015; 98: 50-64. https://doi.org/10.1016/j.supflu.2015.01.002

[20] Amin JS, Kuyakhi HR, Bahadori A. Prediction of formation of polycyclic aromatic hydrocarbon (PAHs) on sediment of Caspian Sea using artificial neural networks. Pet Sci Technol. 2019; 37: 1987-2000. https://doi.org/10.1080/10916466.2018.1496111

[21] Alimohammadi S, Amin JS, Nikooee E. Estimation of asphaltene precipitation in light, medium and heavy oils: experimental study and neural network modeling. Neural Comput Appl. 2017; 28: 679-94. https://doi.org/10.1007/s00521-015-2097-3

[22] Khosravi A, Machado L, Nunes RO. Estimation of density and compressibility factor of natural gas using artificial intelligence approach. J Pet Sci Eng. 2018; 168: 201-16. https://doi.org/10.1016/j.petrol.2018.05.023

[23] Rajabi Kuyakhi H, Boldaji RT, Azadian M. Light hydrocarbons solvents solubility modeling in bitumen using learning approaches. Pet Sci Technol. 2021; 39: 115-31. https://doi.org/10.1080/10916466.2020.1863986

[24] Ghiasi MM, Mohammadi AH, Zendehboudi S. Modeling stability conditions of methane Clathrate hydrate in ionic liquid aqueous solutions. J Mol Liq. 2021; 325, 114804. https://doi.org/10.1016/j.molliq.2020.114804

[25] Ghiasi MM, Yarveicy H, Arabloo M, Mohammadi AH, Behbahani RM. Modeling of stability conditions of natural gas clathrate hydrates using least squares support vector machine approach. J Mol Liq. 2016; 223: 1081-92. https://doi.org/10.1016/j.molliq.2016.09.009

[26] Ghiasi MM, Mohammadi AH. Rigorous modeling of CO_2 equilibrium absorption in MEA, DEA, and TEA aqueous solutions. J Nat Gas Sci Eng. 2014; 18: 39-46. https://doi.org/10.1016/j.jngse.2014.01.005

[27] Kardani N, Bardhan A, Roy B, Samui P, Nazem M, Armaghani DJ, *et al*. A novel improved Harris Hawks optimization algorithm coupled with ELM for predicting permeability of tight carbonates. Eng Comput. 2022; 38: 4323-46. https://doi.org/10.1007/s00366-021-01466-9

[28] Bi J, Bennett KP. Regression Error Characteristic Curves. In: Fawcett T, Mishra N, Eds. Proceedings of the twentieth international conference on machine learning, August 21-24, 2003, Washington, DC, Menlo Park, California: The AAAI Press; 2003, pp. 43-50.

[29] Amin JS, Nikkhah S, Veiskarami M. A statistical method for assessment of the existing correlations of hydrate forming conditions. J Energy Chem. 2015; 24: 93-100. https://doi.org/10.1016/S2095-4956(15)60289-3

[30] Soroush E, Mesbah M, Hajilary N, Rezakazemi M. ANFIS modeling for prediction of CO_2 solubility in potassium and sodium based amino acid Salt solutions. J Environ Chem Eng. 2019; 7(1), 102925. https://doi.org/10.1016/j.jece.2019.102925

[31] Kuyakhi HR, Zarenia O, Boldaji RT. Hybrid intelligence methods for modeling the diffusivity of light hydrocarbons in bitumen. Heliyon 2020; 6(9): e04936. https://doi.org/10.1016/j.heliyon.2020.e04936

[32] Sayyad Amin J, Alimohammadi S, Zendehboudi S. Systematic investigation of asphaltene precipitation by experimental and reliable deterministic tools. Can J Chem Eng. 2017; 95: 1388-98. https://doi.org/10.1002/cjce.22820

[33] Golsefatan A, Shahbazi K. Predicting the effect of nanocomposites on asphaltene removal using a comprehensive approach. Pet Sci Technol. 2020; 38: 64-73. https://doi.org/10.1080/10916466.2019.1656241

[34] Pan W. Akaike's information criterion in generalized estimating equations. Biometrics. 2001; 57: 12055. https://doi.org/10.1111/j.0006-341X.2001.00120.x

[35] Bonakdari H, Binns AD, Gharabaghi B. A comparative study of linear stochastic with nonlinear daily river discharge forecast models. Water Resour Manag. 2020; 34: 3689-708. https://doi.org/10.1007/s11269-020-02644-y